JOURNAL OF AIRCRAFT
Vol. 30, No. 6, Nov.–Dec. 1993

Forward Flight Trim and Frequency Response Validation of a Helicopter Simulation Model

Frederick D. Kim* and Roberto Celi†
University of Maryland, College Park, Maryland 20742
and
Mark B. Tischler‡
NASA Ames Research Center, Moffett Field, California 94035

This article describes a new trim procedure that includes the calculation of the steady-state response of the rotor blades and is applicable to straight flight and steady coordinated turns. This article also describes the results of a validation study for a high-order linearized model of helicopter flight dynamics that includes rotor, inflow, and actuator dynamics. The model is obtained by numerical perturbations of a nonlinear, blade element-type mathematical model. Predicted responses are compared with flight test data for two values of airspeed. The comparison is carried out in the frequency domain. Numerical simulations and comparisons with flight test data show that the trim algorithm is accurate and preserve the periodicity of the aircraft states. The results also indicate that the predictions of the on-axis frequency response are overall in good agreement with flight test data, especially at medium and high frequencies.

Nomenclature

C_T = thrust coefficient
$[F]$ = linearized system matrix
g = acceleration due to gravity
$[G]$ = linearized control matrix
G_{xx}, G_{yy}, G_{xy} = input, output, and cross-spectral density
m = aircraft mass
p, q, r = angular velocity components about body axes
u, v, w = velocity components along body axes
$\boldsymbol{u}$ = control vector
V = airspeed
X = aerodynamic force along x-body axis
y_0, y_{kc}, y_{ks} = harmonics of rotor blade response
y_{NR} = state vector in nonrotating system
y_R = state vector with rotor states in rotating system
α, β = fuselage aerodynamic incidence and sideslip
γ_{xy} = coherence function
δ_{col} = collective pitch input, in.
δ_{lat}, δ_{lon} = lateral and longitudinal control inputs, in.
δ_{ped} = directional control input, in.
ζ = damping ratio
θ_0, θ_t = collective pitch of main and tail rotor, rad
θ_{1c}, θ_{1s} = cyclic pitch components of main rotor, rad
λ = main rotor inflow
λ_0, λ_{1c}, λ_{1s} = harmonics of dynamic inflow for main rotor
μ = advance ratio
ν_e = rotor induced downwash at the tail
ν_0 = total rotor downwash, nondimensional
ϕ, θ, ψ_B = fuselage attitudes, Euler angles
ψ = blade azimuth angle
Ω = main rotor speed
ω = undamped natural frequency, rad/s
$(\dot{})$ = derivative with respect to time
$\Delta(\ldots)$ = small perturbation quantity

Subscripts
HP = hub plane
NR = quantity in the nonrotating system

Received March 8, 1991; revision received July 2, 1992; accepted for publication Aug. 20, 1992.

*Army Rotorcraft Fellow, Center for Rotorcraft Education and Research, Department of Aerospace Engineering; currently Aerospace Engineer, NASA Ames Research Center.
†Assistant Professor, Center for Rotorcraft Education and Research, Department of Aerospace Engineering. Member AIAA.
‡Army Rotorcraft Group Leader, U.S. Army Aeroflightdynamics Directorate. Member AIAA.

Introduction

IN recent years there has been increasing interest in high-gain, full-authority helicopter flight control systems as a means of satisfying new, stringent handling qualities requirements.[1] An important ingredient necessary for the development of these advanced flight control systems is an accurate, linear time invariant mathematical model of the flight dynamics of the helicopter. To maintain its accuracy over a sufficiently wide frequency band, such a model must be of high enough order to represent the rotor and the inflow dynamics. A review of the state of the art for the formulation of high-order helicopter simulation models has been presented in Ref. 2. In the context of this study, a "simulation" mathematical model is one that allows the prediction of the stability and control characteristics of a helicopter; models obtained using system identification techniques from flight test data are not included.

In many studies, simulation models are validated in the time domain through comparisons with time histories from flight tests. Recently, studies based on frequency domain methods have provided a more comprehensive picture of the validity of rotorcraft simulation models. Ballin[3] used frequency responses obtained from hover flight data to validate the Ames-Genhel simulation of the UH-60, and demonstrated the importance of inflow modeling for good dynamic response prediction. For the case of forward flight (of interest in this study) the only published frequency domain validation appears to be that of Kaplita et al.[4] Comparisons with flight test data were presented for a CH-53 helicopter flying at 70 kt. An elastic fuselage and an external suspended load were in-

cluded in the model, which had a total of 42 states. Good correlation was observed in the frequency band from about 2 rad/s to 15–20 rad/s. Some discrepancies were observed around the frequency of the lag regressive mode, and tentatively attributed to the modeling of the lag dampers and to blade flexibility.

The linear models are generally obtained through analytical or numerical linearization of a set of nonlinear equations of motion of the helicopter about a steady-state equilibrium, or trim, condition. When a forward flight condition is considered, and when rotor and inflow dynamics are included in the model, the trim problem requires particular care. The steady-state equilibrium of a helicopter is rigorously described by a mixed set of algebraic and differential equations, that model the dynamics of the rotor and of the fuselage, as well as certain kinematic relationships that must hold true in trimmed flight. Because mixed differential-algebraic systems of equations cannot presently be solved reliably, at least for systems of the complexity required for helicopter flight dynamics applications, some approximations need to be introduced to split the algebraic and the differential equation portions of the problem.

In the current literature, there are various approaches to the problem of finding the equilibrium solution of a helicopter in flight.

The trim procedure used in the Genhel simulation program[5] is based on adjusting the four pilot controls, plus angle of attack and sideslip angles of the aircraft based on the integral of the error between the actual and the desired values of the aircraft translational and rotational accelerations. Because the aircraft is "flown" numerically into a trim condition, the steady-state, periodic motion of the blades at trim is available as a by-product of the algorithm once the trim state has been achieved. A similar philosophy is used by Peters et al.[6,7] in the so-called "autopilot" method. In this method the rotor is trimmed using a simulated feedback controller that continuously adjusts the controls to achieve the desired hub forces and moments. Some care needs to be used in the selection of gains and time constants of the controller in order to ensure the convergence of the algorithm. Another approach consists of using periodic shooting methods to obtain the rotor trim solution.[8] In this method, one iterates on the initial conditions and the controls until a periodic solution is found. References 6–8 focus on straight flight conditions only.

A set of equations describing the trim state of a helicopter in coordinated, steady helical turns was derived by Chen.[9] In Ref. 10, these equations were augmented by a set of nonlinear algebraic equations which describe the steady-state response of the rotor, and which were obtained by applying the Galerkin method to the finite element equations of motion of the blades. The resulting system of nonlinear equations provides the trim state for the complete helicopter and the steady-state blade response. A similar approach is used by Takahashi[11]: the equations of motion of the rotor are transformed into a system of nonlinear algebraic equations using the harmonic balance method, and are combined with the fuselage equations for a coupled trim solution. Alternatively, the rotor equations of motion can be transformed into algebraic equations using a finite element in time approach, as shown by Lim and Chopra.[12] Both Refs. 11 and 12 deal with straight flight conditions only.

This article has the following objectives:

1) To describe an improved procedure for accurate calculations of the trim state of the helicopter. The procedure yields both the value of the trim variables of the aircraft and the steady-state, periodic equilibrium position of the rotor blades. No averaging or filtering of rotor forces and moments is carried out, and the full periodicity of the trim variables is retained. The trim procedure can model straight flight and coordinated turns.

2) To present validation results for a high-order linearized model extracted from a nonlinear, blade element-type model. The linearized model describes the small perturbation motion about a trimmed equilibrium position. The validation is carried out by comparing the frequency response predicted by the linearized model and the frequency response identified from flight test data. Results are presented for two different values of advance ratio.

Validation results for the linearized model of this study, limited to the case of hover, have been presented in Ref. 2. Frequency responses predicted by the linearized model were compared with the frequency responses identified from flight test data and with those identified from nonlinear simulation results and presented in Ref. 3. The validation indicated fair to good agreement for frequencies of up to 1 rad/s, and good to excellent agreement between 1 and 10–15 rad/s. In the region above 15 rad/s, which includes the lowest frequency rotor modes, the linearized model captured most of the dynamics. However, the flight test data in this frequency band were somewhat unreliable.

Mathematical Model

Helicopter Simulation Model

The mathematical model of the helicopter is described in detail in Ref. 2, and only a brief outline will be presented here. The model consists of a nonlinear, blade element-type representation of a single rotor helicopter with a rigid fuselage. No small angle assumptions are invoked for the angles of attack of rotor and fuselage. Therefore, the model is valid for a wide range of fuselage attitudes. The main rotor blades are individually modeled as rigid bodies undergoing flap and lag motion. An empirical correction for the dynamic twist due to the torsional dynamics of the blades is also included. A three-state[13] and a one-state dynamic inflow model are used for the main rotor and the tail rotor, respectively. Aerodynamic forces are calculated using blade element theory with table lookup for lift and drag coefficients. The aerodynamics of the fuselage and the empennage is modeled using tables of aerodynamic coefficients obtained from wind-tunnel tests. The equations of motion of the fuselage are formulated and solved in a fixed system of body axes. The equations of motion of the rotor are formulated and solved in a rotating coordinate system. A rotating-to-fixed coordinate transformation is carried out for the rotor variables, therefore, the entire output of the computer program implementing the model is in the body fixed coordinate system. No particular emphasis was placed on real-time execution requirements. Therefore, although the model lends itself to very efficient computer implementations, it should be considered as a mathematical model for off-line, nonreal-time flight dynamics simulations.

A linearized set of small perturbation equations of motion can be extracted from the nonlinear model. The coefficients of the model are obtained numerically, using finite difference approximations. The order of the system is 32. Additionally, the dynamics of each of the four pitch control actuators can be represented by a second-order transfer function. Therefore, another eight states can be appended to the linearized model, for a total overall size of 40 states.

Coupled Rotor-Fuselage Trim

In the calculation of the trim state of the fuselage, the full periodicity of the forces and moments generated by the rotor blades is retained. No averaging or filtering of such forces and moments is used. Therefore, the fuselage motion quantities are generally composed of a steady-state value, with superimposed a smaller, n/rev periodic variation. The coupled trim problem, which includes the determination of the steady-state, periodic motion of the rotor blades, consists of two phases.

Phase I—Algebraic Solution

The first phase is based on a set of equations describing the kinematics of a helicopter undergoing a coordinated, steady,

helical turn. These equations were originally developed by Chen[9] and were extended in Ref. 10 to include the steady-state response of the rotor. They are modified further in this study, to take into account the periodicity of both rotor and fuselage motion. A set of 16 algebraic equations describes the trim state of the entire aircraft. Additional algebraic equations, in a number that depends on the required accuracy, describe the steady-state motion of the rotor blades.

1) Force and moment equilibrium: These equations are substantially identical to those written in the more traditional form in which force and moment resultants appear explicitly, but proved easier to implement in the mathematical model of this study. For example, instead of enforcing the following X-force equilibrium equation:

$$X = mg \sin \theta + m(qw - rv) \tag{1}$$

the equivalent condition is used

$$\int_0^{2\pi} \dot{u}\, d\psi = 0 \tag{2}$$

It should be noted that when the n/rev variation of the fuselage motion quantities u, v, w, p, q, and r are taken into account, the corresponding time derivatives are equal to zero only in an average sense, as implied in Eq. (2). Similar conditions are enforced on $\dot{v}$, $\dot{w}$, $\dot{p}$, $\dot{q}$, and $\dot{r}$ for a total of five additional equations.

2) Requirements on the Euler rates of the fuselage: The Euler rates for the fuselage are also equal to zero only in an average sense. A condition similar to Eq. (2) is therefore enforced on $\dot{\theta}$, $\dot{\phi}$, and $(\dot{\psi}_B - \dot{\psi}_B)$, where $\dot{\psi}_B$ is the prescribed turn rate, assumed constant, that defines the turning flight condition.

3) Kinematic relationships for roll attitude:

$$\int_0^{2\pi} \left[\sin \phi - \frac{\dot{\psi}_B V}{g} (\cos \alpha \cos \phi + \sin \alpha \tan \theta) \cos \beta \right] d\psi = 0 \tag{3}$$

For advance ratios less than 0.1, this equation is not used. The sideslip angle β is set to zero, and the aircraft trims to a variable roll attitude.

4) Relationships between aerodynamic angle-of-attack α and pitch attitude angle θ:

$$\cos \alpha \cos \beta \sin \theta - (\sin \beta \sin \phi + \sin \alpha \cos \beta \cos \phi) \cos \theta = \sin \gamma \tag{4}$$

5) Requirements on time derivatives of the harmonics of dynamic inflow for main rotor:

$$\int_0^{2\pi} \dot{\lambda}_0\, d\psi = 0 \tag{5}$$

$$\int_0^{2\pi} \dot{\lambda}_{1c} \cos \psi\, d\psi = 0 \tag{6}$$

$$\int_0^{2\pi} \dot{\lambda}_{1s} \sin \psi\, d\psi = 0 \tag{7}$$

6) Tail rotor inflow and delay of downwash effects on the tail:

$$\int_0^{2\pi} \left(\lambda_t + \mu \tan \alpha_{HPt} + \frac{C_{Tt}}{\sqrt{\mu^2 + \lambda_t^2}} \right) d\psi = 0 \tag{8}$$

$$\nu_e = \nu_0 \tag{9}$$

7) Azimuthwie Galerkin solution of the equations of motion of the blade: This additional set of equations describes the steady-state motion of the blades. A detailed description can be found in Ref. 14. First, the vector of generalized coordinates that describe the motion of the blade is approximated by a truncated Fourier series

$$y \approx y_{app} = y_0 + \sum_{k=1}^{n} (y_{kc} \cos k\psi + y_{ks} \sin k\psi) \tag{10}$$

Then the approximate solution y_{app} is substituted into the equation of motion of the blade $F(y, \dot{y}, \ddot{y}; \psi) = 0$, and the following conditions are enforced on the residual:

$$\int_0^{2\pi} F(y_{app}, \dot{y}_{app}, \ddot{y}_{app}; \psi)\, d\psi = 0 \tag{11}$$

$$\int_0^{2\pi} F(y_{app}, \dot{y}_{app}, \ddot{y}_{app}; \psi) \cos k\psi\, d\psi = 0 \tag{12}$$

$$\int_0^{2\pi} F(y_{app}, \dot{y}_{app}, \ddot{y}_{app}; \psi) \sin k\psi\, d\psi = 0 \tag{13}$$

$$k = 1, 2, \ldots, n$$

The study presented in this article concerns an articulated rotor. Therefore, the rigid blade flap and lag angles, and the dynamic twist variables[2] are used as generalized coordinates. For all the results presented, $n = n_F = 2$ for flap, $n = n_L = 2$ for lag, and $n = n_T = 1$ for the dynamic twist correction.

Equations (2–13) represent a set of $16 + (2n_F + 1) + (2n_L + 1) + (2n_T + 1)$ nonlinear algebraic equations. The vector of unknowns is composed of main and tail rotor pitch settings, aerodynamic incidence and sideslip, fuselage roll, pitch, and yaw rates, pitch and roll attitudes, main and tail rotor inflow components, and the coefficients of the Fourier expansion in Eq. (10) for the flap, lag, and twist degrees of freedom (DOF). Further details on the implementation of the algorithm can be found in Ref. 15.

Phase II—Shooting Method

If needed, the trim solution obtained as described above can be further refined using the algorithm described in this section, based on a shooting method. This technique enforces the correct periodicity, as well as the average trim of the phase I solution.

The algorithm consists of selecting a vector $\boldsymbol{X}$ of unknowns, defined as

$$\boldsymbol{X} = [\theta(0)\ \phi(0)\ \theta_0\ \theta_{1c}\ \theta_{1s}\ \theta_t\ p(0)\ q(0)\ r(0)\ y_0^T\ y_{1c}^T \ldots y_{nc}^T\ y_{1s}^T \ldots y_{ns}^T]^T \tag{14}$$

such that the state vector

$$\boldsymbol{Y}(\psi) = [u\ v\ w\ p\ q\ r\ \phi\ \theta\ \psi_B\ \dot{y}_{app}^T\ y_{app}^T]^T \tag{15}$$

has identical values at $\psi = 0$, and after a given number n of rotor revolutions, that is

$$\boldsymbol{R} = \boldsymbol{Y}(\psi = 0) - \boldsymbol{Y}(\psi = 2n\pi) = 0 \tag{16}$$

For all the results presented in this article $n = 1$. The initial guesses for the vector $\boldsymbol{X}$ and the vector $\boldsymbol{Y}(0)$ are given by the final results of phase I. The values of $u(0)$, $v(0)$, $w(0)$, and $\psi_B(0)$ are maintained fixed in phase II, and equal to the value at the end of phase I. This is essentially equivalent to maintaining the angle-of-attack α and the sideslip β constant, at the values these quantities had at the end of phase I. The equations of motion are then integrated from $\psi = 0$ to $\psi =$

$2n\pi$, and the residual vector $\boldsymbol{R}$ is calculated from Eq. (16). It is interesting to point out that a different form of vector $\boldsymbol{X}$ was initially selected in this study: the vector contained the initial conditions $u(0)$, $v(0)$, $w(0)$ and $\psi_B(0)$, and the pitch settings were maintained fixed at the values provided by phase I. The convergence of phase II using this vector proved erratic, and at least one order of magnitude more expensive computationally, compared with the cases in which the form of Eq. (14) was used.

Equation (16) represents a system of nonlinear algebraic equations in the unknown vector $\boldsymbol{X}$, the solution of which completes the set of initial conditions for the equations of motion of the helicopter.

Linearized Model in Forward Flight

The linear model is obtained by numerical linearization of the nonlinear model about the trim condition, as explained in detail in Ref. 2. The hover dynamics is generally described by a system of differential equations with constant coefficients. Therefore, the coefficients of the linearized model will not depend on the blade azimuth angle at which the linearization is carried out. On the other hand, the linearized forward flight model has periodic coefficients, which will vary depending on the blade azimuth angle. The linearization of the rotor equations is carried out in the rotating coordinate system. A multiblade coordinate transformation converts the linearized information to the fixed frame.[2] In the case of forward flight, such a transformation reduces, but does not completely eliminate, the periodicity of the system. Therefore, an approximate constant coefficient representation is obtained by carrying out the linearization at a certain number of points along the blade azimuth and then averaging the results. The resulting linear, constant coefficient system is

$$\Delta\dot{\boldsymbol{y}}_{\mathrm{NR}} = [F_{\mathrm{avg}}]\Delta\boldsymbol{y}_{\mathrm{NR}} + [G_{\mathrm{avg}}]\Delta\boldsymbol{u} \tag{17}$$

where

$$[F_{\mathrm{avg}}] = \frac{1}{N}\sum_{i=1}^{N}[F(\psi_i)] \qquad [G_{\mathrm{avg}}] = \frac{1}{N}\sum_{i=1}^{N}[G(\psi_i)] \tag{18}$$

with $\psi_i = 2\pi i/N$. For all the results presented in this article, $N = 12$.

Results

This section is divided into two parts. The first part presents results that illustrate the characteristics of the trim algorithm. Although the trim state can be calculated for straight as well as turning flight conditions, only results for straight flight will be presented here. The second part contains results of a validation study in which the frequency response predicted by the linearized model is compared with that identified from flight tests. All the results refer to a UH-60 helicopter, flying at a gross weight of 15,334 lb.

Trim in Forward Flight

Table 1 lists the values of controls and selected states after each phase, and shows that the results of the first phase of the trim procedure are very close to those of the complete procedure. A complete phase I trim calculation requires about 2 min of CPU time, whereas a complete phase II trim calculation requires about 5 min when periodicity is enforced after one rotor revolution (the CPU times refer to a Sun 3/280 workstation, with speed of about 0.5 LINPACK MFlops). The phase II results presented were obtained by enforcing periodicity after one rotor revolution.

Table 1 Comparison of selected trim results at 120 kt

Variable	Phase I	Phase II	Error, %
Lateral, deg	−0.2862	−0.2850	0.42
Longitudinal, deg	9.2307	9.2306	0.001
Collective, deg	18.4909	18.4910	0.001
Tail rotor collective, deg	11.8685	11.8684	0.001
Roll attitude, deg	0.0	0.0	0.0
Pitch attitude, deg	0.6488	0.6492	0.06
Main rotor inflow	0.009681	0.009671	0.01
Tail rotor inflow	0.01612	0.01612	0.0

The trim procedure described in this article preserves the full periodicity of both the rotor and the fuselage response. The upper plot in Fig. 1 shows the time history of the vertical velocity w starting from a trim condition, and maintaining the controls fixed at their trim values. In the scale of the figure, the time history appears to be a straight line. Expanding greatly the ordinate scale, however, reveals that the time history is actually composed of a predominant steady-state value, with a superimposed small n/rev oscillation, as shown in the lower portion of the Fig. 1, due to the small n/rev variations of hub forces and moments. A similar behavior occurs for all the fuselage-related states.[15]

Figures 2–5 present a comparison of calculated trim conditions with the flight test results of Ref. 16. The overall accuracy of the predictions is good throughout the range of airspeeds considered in the figures. Figure 2 shows that collective pitch and required main rotor power are underpredicted below 50 kt, corresponding to $\mu = 0.11$, probably due to the relatively crude main rotor inflow model. This can also explain the underprediction of lateral cyclic pitch at low speed, shown in Fig. 3. The shape of the analytical curves for roll attitude (Fig. 3) and sideslip (Fig. 5) is due to the choice of arbitrarily setting the sideslip angle to zero and letting the roll attitude vary, for an advance ratio $\mu < 0.1$, and setting the roll attitude to zero for $\mu \geq 0.1$ with a variable sideslip angle. The pedal position required for trim is underpredicted by 5–10% of the full control excursion at all speeds. The agreement between theoretical and experimental data is very similar to that of Ref. 17, in which the correlation study was carried out

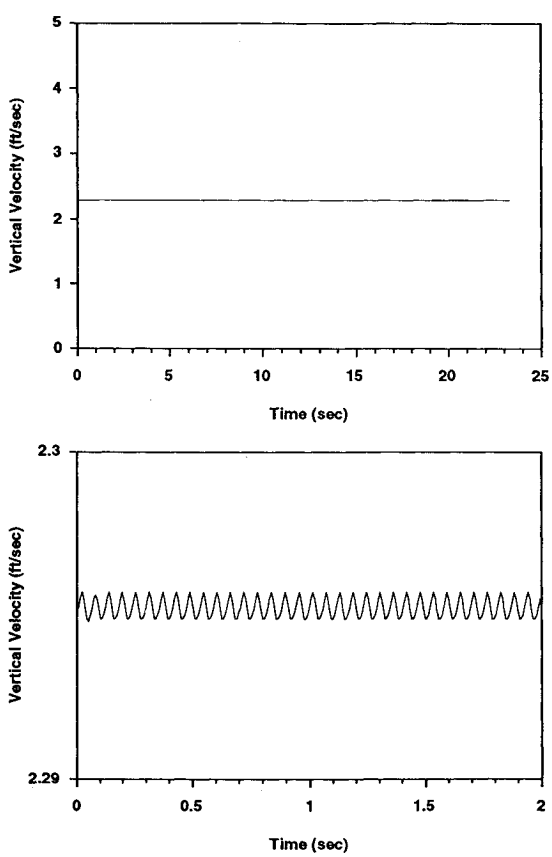

Fig. 1 Time history of vertical velocity for trimmed helicopter; V = 120 kt.

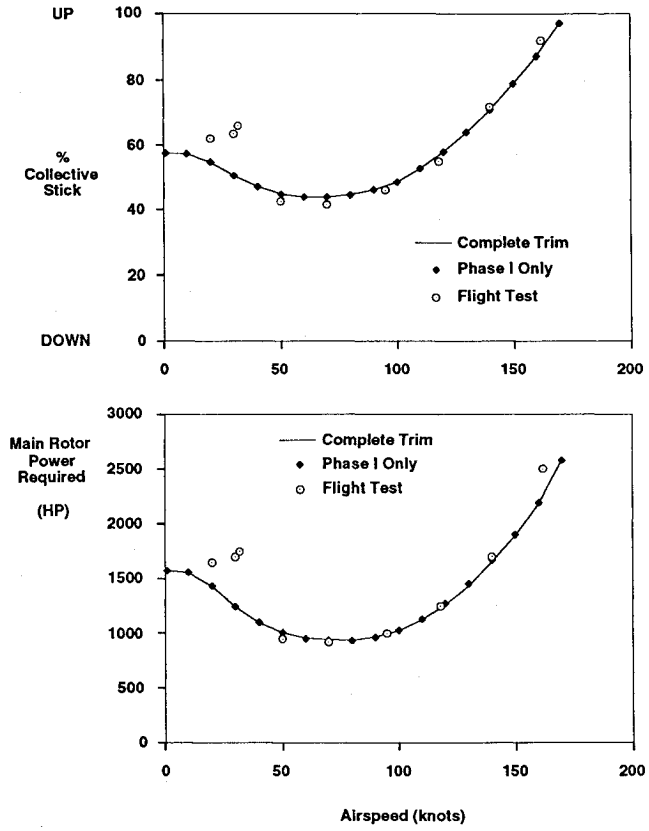

Fig. 2 Collective pitch and required power at trim.

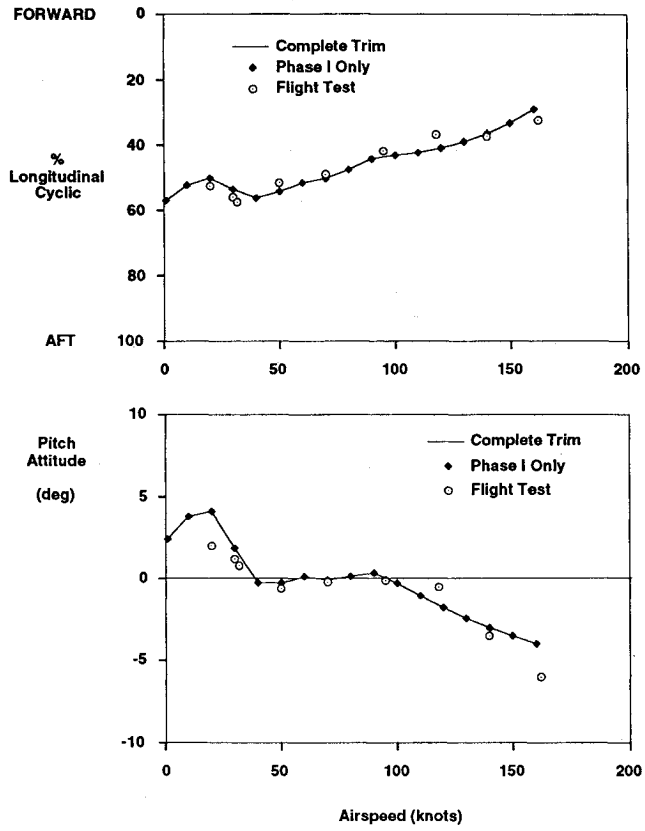

Fig. 3 Longitudinal cyclic pitch and pitch attitude at trim.

using the original version of Genhel. Blade motion were not available, therefore, the correlation of these quantities could not be evaluated. Finally, Figs. 2–5 clearly indicate that there is no discernible increase in accuracy when the results of phase I of the trim procedure are refined with the shooting method procedure of phase II. The refinement may be useful for rotor configurations or flight conditions in which an accurate evaluation of the elastic response of the blades is important.

Frequency Response

This section presents the results of a validation study for the linearized mathematical model, and for forward flight conditions. The on-axis, bare airframe frequency response predicted by the model is compared with the bare airframe frequency response identified from flight tests. A similar comparison for a hover flight condition was presented in Ref. 2.

The flight tests were carried out at speeds $V = 80$ kt and $V = 120$ kt, corresponding to $\mu = 0.19$ and $\mu = 0.28$, respectively. The flight path was straight and horizontal, therefore, both the yaw rate and the flight path angle were equal to zero. General information on the testing techniques, and on the theoretical background for the procedure used to identify the frequency response data, is available in Ref. 18. Additional information on the frequency response identification procedure can be found in Ref. 3, in which this technique was applied to identification from off-line computer simulation data, applied to a UH-60 in hover.

For each flight condition, four sets of Bode plots compare the predicted and the identified on-axis frequency responses: roll rate due to lateral cyclic, pitch rate due to longitudinal cyclic, yaw rate due to pedal, and vertical acceleration due to collective pitch. Each Bode plot pair contains an indication of the range of frequencies for which the flight test data are considered sufficiently accurate. The reliability of the flight test frequency responses at a given frequency is evaluated based on the value of the coherence function γ_{xy} at the frequency, defined as

$$\gamma_{xy}^2 = (G_{xy}^2/G_{xx}G_{yy}) \tag{19}$$

The role of the coherence function in the evaluation of frequency response identification results is discussed extensively in Ref. 19. The frequency band marked in the plots as "accurate flight test data" is that for which $\gamma_{xy}^2 \geq 0.6$. The curves marked "UM-Genhel" show the response predicted by the linearized model of this study. The curves marked "with engine" were obtained by adding six states to model the rotor speed DOF and the propulsion system dynamics, as well as a model of the engine governor. This improved model will be described in detail in a forthcoming publication.[20] Its results are included here to clarify some aspects of the low-frequency behavior of the model of the present study.

It should be pointed out that the main objectives for the mathematical model described in this article are to help predict compliance with handling qualities specifications and, in particular, to support the design of advanced flight control systems. Therefore, the frequency range of particular interest goes from about 1 rad/s to about 10–15 rad/s, and the processing of the flight test data was carried out so as to maximize the coherence in this frequency range.

In all the plots, the units for angular rates and accelerations are deg/s and g, respectively. The input unit is an inch of pilot stick. Because of the presence of a control mixer, correction factors are needed to convert from swashplate inputs to "unmixed" pilot stick inputs. These factors, as well as other details of the pitch control system modeling, can be found in Ref. 15.

Table 2 lists the poles of the helicopter in forward flight. For clarity, the table separates the fuselage and the aerodynamic modes from the rotor modes. At 80 kt, there are a total of nine fuselage poles. They are identified as the phugoid (two complex conjugate poles), Dutch roll (two), short-period (two), spiral (one real pole), lateral velocity (one), and yaw (one). The pole at the origin for yaw is the direct consequence of retaining heading as one of the states in the model. At 120 kt, the phugoid poles coalesce and split into two real poles, corresponding to aperiodic modes. In addition, the lateral velocity mode appears to couple with the main rotor inflow, and the respective poles merge into a pair of complex con-

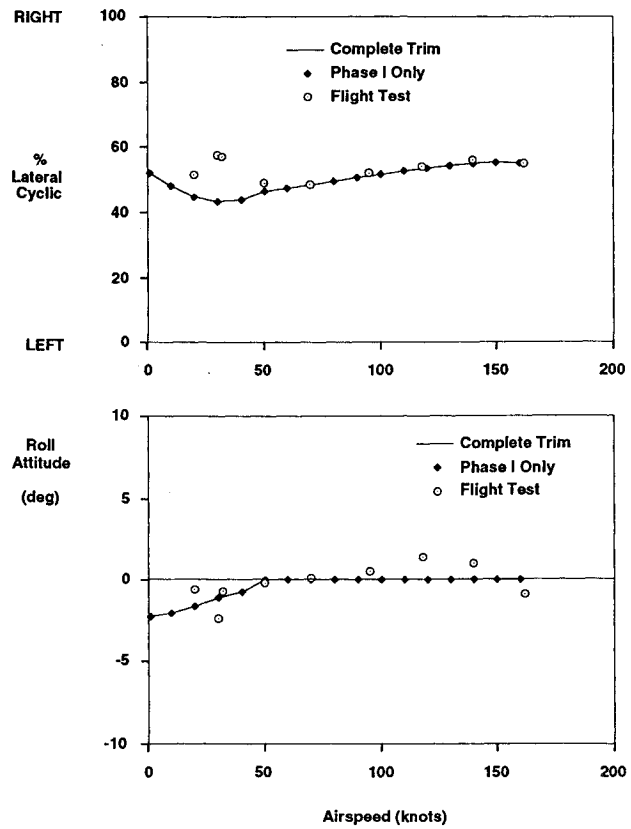

Fig. 4 Lateral cyclic pitch and roll attitude at trim.

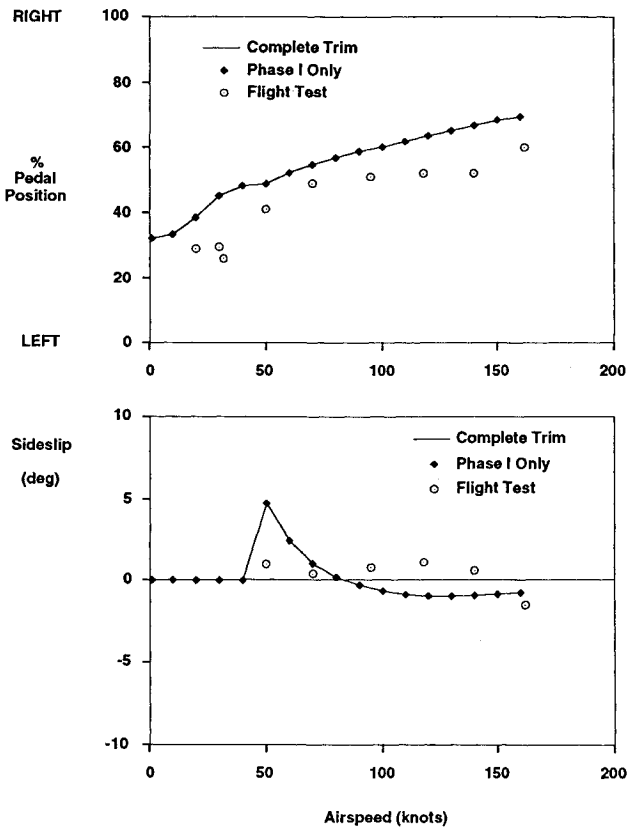

Fig. 5 Pedal position and sideslip angle at trim.

jugate poles. Another interesting observation is the behavior of the harmonic components of the dynamic inflow. At 80 kt, poles of the sine and the cosine components form a complex conjugate pair. On the other hand, at 120 kt, they split into two stable aperiodic modes. A total of nine complex conjugate pole pairs describe the rotor modes listed in the table: four for flap, four for lag, and one for torsion. The flap and lag modes include the collective, progressive, regressive, and reactionless modes. The lightly damped regressive lag mode ($\zeta = 0.18$, $\omega = 18.3$ for $V = 80$ kt) plays a key role in limiting the achievable roll response bandwidth, as discussed in Ref. 18. Torsion was formulated as a common dynamic twist model for all four blades and yields only one periodic mode.

Figures 6 and 7 show the role rate response at $V = 80$ kt and $V = 120$ kt, respectively. The figures indicate that amplitude and phase are well predicted at both speeds, especially for frequencies above 1–2 rad/s. The notch-type response and the phase increase associated with the regressive lag mode of the main rotor are captured correctly by the model. Discrepancies in both amplitude and phase predictions appear below 1–2 rad/s for the amplitudes, and 0.4–0.5 rad/s for the phase. In particular, the linearized model predicts rather large phase delays at low frequency, which are not observed in flight.

Figures 8 and 9 show the pitch rate response to longitudinal cyclic at $V = 80$ kt and $V = 120$ kt, respectively. As for the roll rate case, the predicted and measured responses are in good agreement above 1–2 rad/s for both amplitude and phase. The agreement remains good even at 20–30 rad/s, although the low coherence makes the reliability of the flight test data above 12–15 rad/s questionable. Below 0.5 rad/s, the correlation is worse, and again much larger phase delays are predicted that are not observed in flight.

The yaw rate responses to pedal input at $V = 80$ kt and $V = 120$ kt are shown respectively in Figs. 10 and 11. For this axis, the responses identified from flight tests are reliable only from about 2 rad/s to about 12–13 rad/s. In this frequency band the predictions of the linearized model are reasonably accurate for both values of speed. Below 2 rad/s, fairly large discrepancies are observed in both amplitude and phase. Above 15 rad/s, increases in amplitude and phase indicated by the flight test data are not captured by the analytic predictions. For these low- and high-frequency cases, however, no conclusive statement can be made because of the low coherence values.

Finally, Figs. 12 and 13 show the vertical acceleration response to collective at $V = 80$ kt and $V = 120$ kt, respectively. The frequency response data from the flight test at 80 kt are reliable between 0.7 and 22–24 rad/s. Over this entire frequency range the theoretical model overpredicts the ampli-

Table 2 Poles of the helicopter at 80 and 120 kt

Mode	80 kt	120 kt
Phugoid	[−0.1912, 0.7803]	(−0.1293)
Phugoid		(0.0801)
Dutch roll	[0.09490, 0.2150]	[−0.1890, 0.7492]
Yaw	(0)	(0)
Spiral	(0.5982)	(0.6643)
Short-period	[0.9899, 1.615]	[0.9647, 1.637]
Lateral velocity	(2.157)	[0.8683, 3.776]*
Main rotor inflow	(3.603)	[0.8683, 3.776]*
Main rotor inflow, sin	[0.8571, 14.74]*	(30.02)
Main rotor inflow, cos	[0.8571, 14.74]*	(51.33)
Tail rotor inflow	(64.82)	(93.66)
Delayed downwash	(142.9)	(142.9)
Collective lag	[0.5105, 7.913]	[0.5216, 7.764]
Reactionless lag	[0.5660, 8.221]	[0.7146, 9.135]
Regressive lag	[0.1757, 18.25]	[0.2101, 18.53]
Collective flap	[0.3354, 26.34]	[0.2908, 26.97]
Reactionless flap	[0.4500, 27.78]	[0.4583, 27.39]
Regressive flap	[0.9944, 34.27]	[0.9849, 19.33]
Progressive lag	[0.1084, 37.63]	[0.1181, 37.33]
Progressive flap	[0.2247, 51.84]	[0.2190, 52.22]
Dynamic twist	[0.2854, 172.3]	[0.2819, 180.2]

[ζ, ω] implies [$s^2 + 2\zeta\omega s + \omega^2$], and (a) implies ($s + a$). An asterisk implies "members of the same complex conjugate pair."

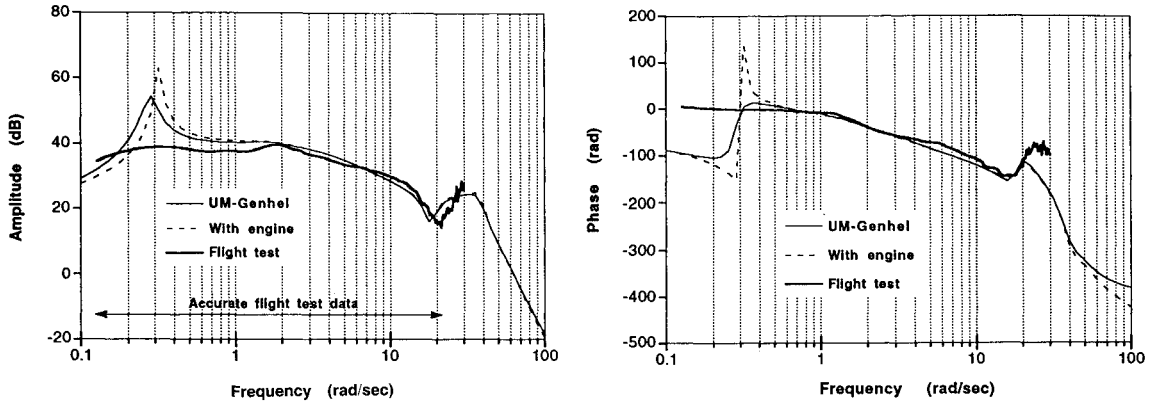

Fig. 6 Roll rate frequency response to lateral cyclic input δ_{lat}; $V = 80$ kt.

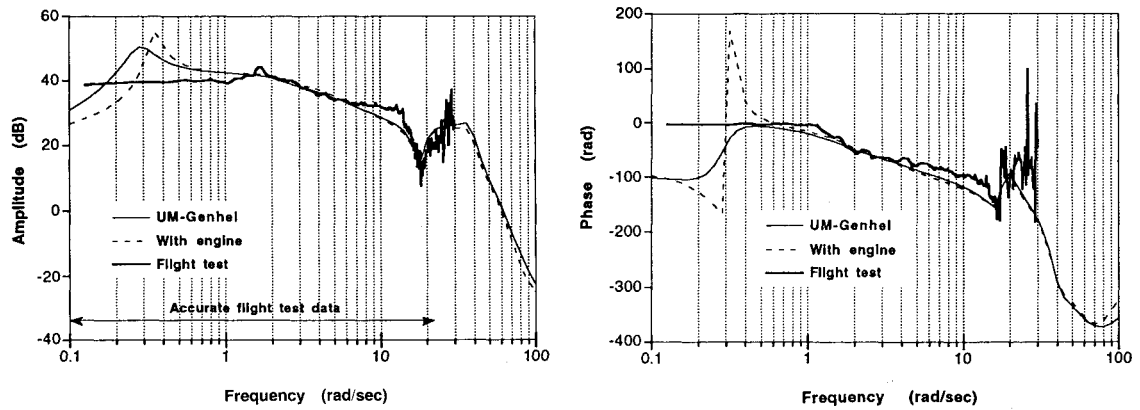

Fig. 7 Roll rate frequency response to lateral cyclic input δ_{lat}; $V = 120$ kt.

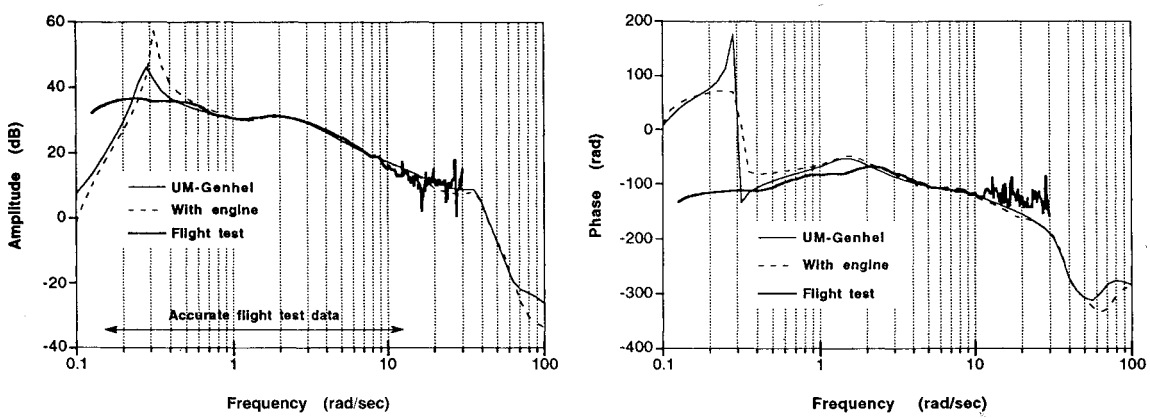

Fig. 8 Pitch rate frequency response to longitudinal cyclic input δ_{lon}; $V = 80$ kt.

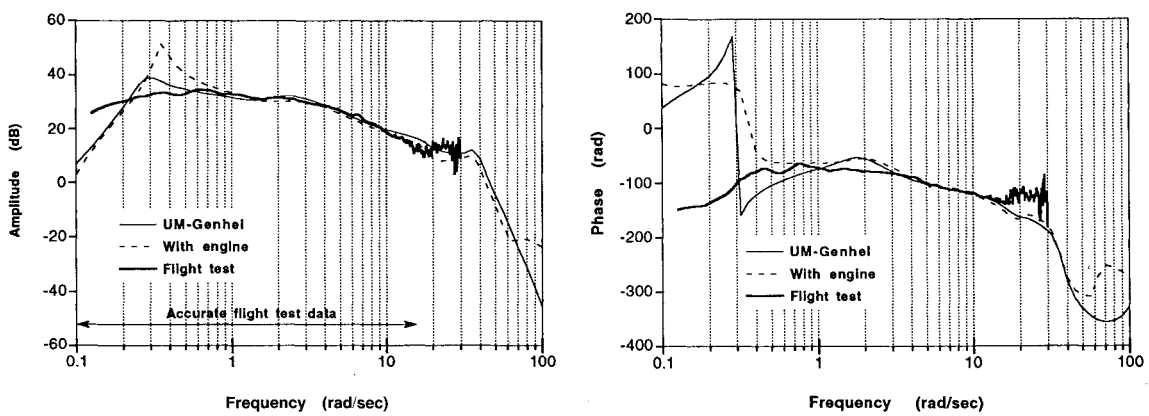

Fig. 9 Pitch rate frequency response to longitudinal cyclic input δ_{lon}; $V = 120$ kt.

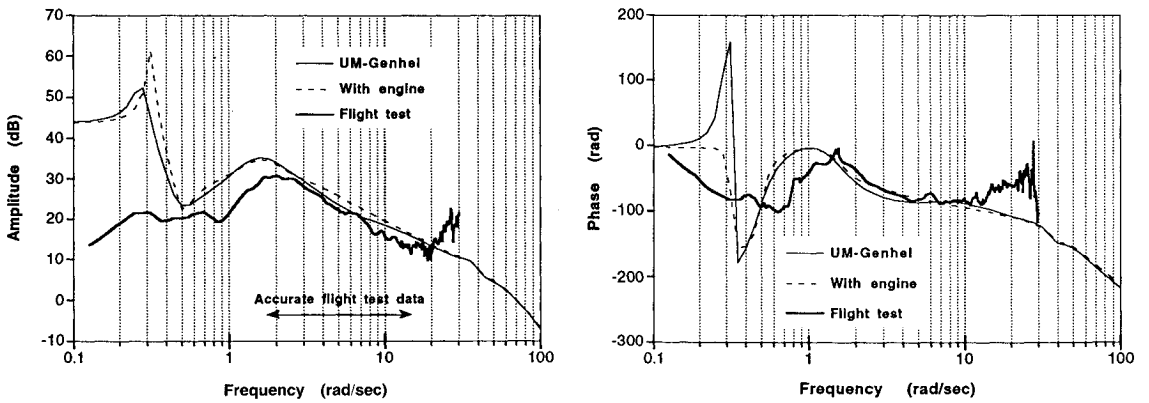

Fig. 10 Yaw rate frequency response to pedal input δ_{ped}; V = 80 kt.

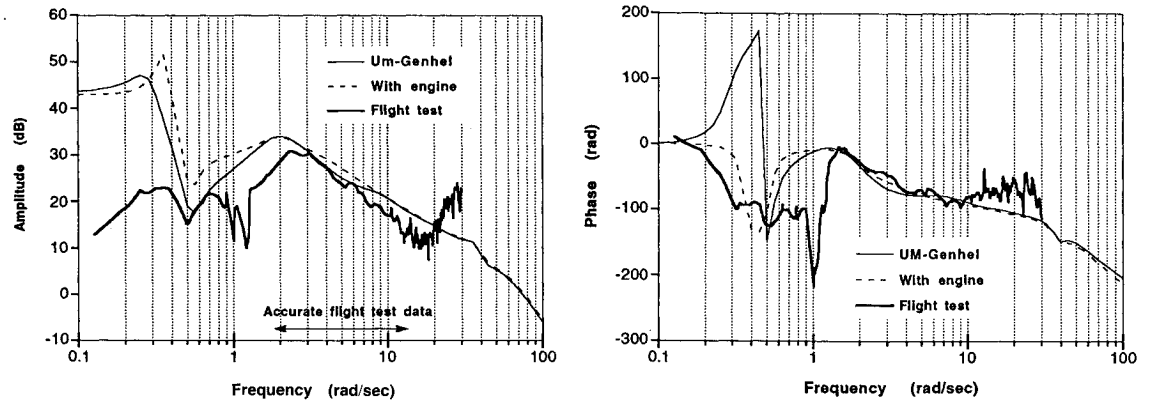

Fig. 11 Yaw rate frequency response to pedal input δ_{ped}; V = 120 kt.

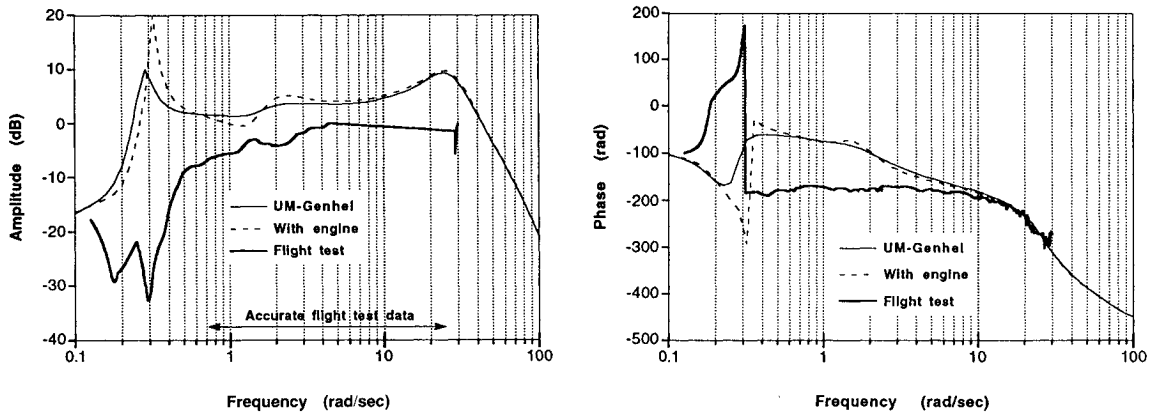

Fig. 12 Vertical acceleration frequency response to collective pitch input δ_{col}; V = 80 kt.

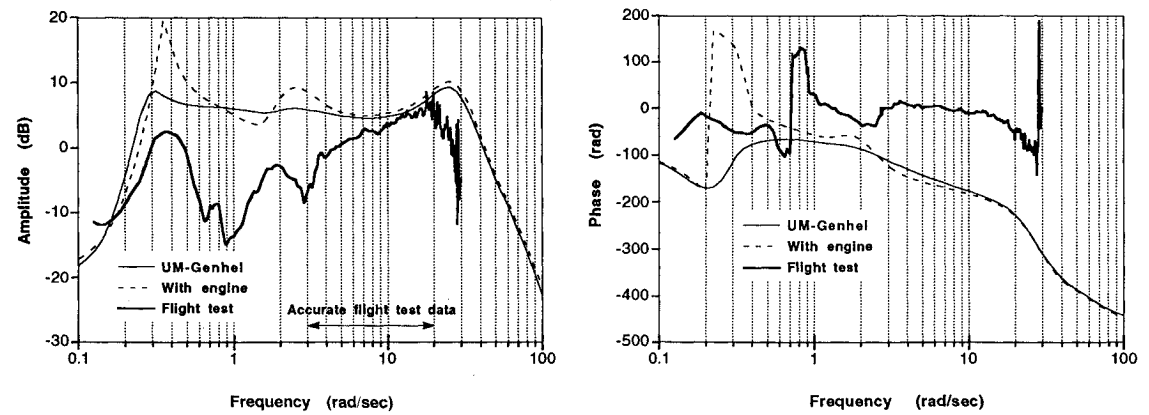

Fig. 13 Vertical acceleration frequency response to collective pitch input δ_{col}; V = 120 kt.

tude of the response by 5–10 dB. The phase delay is underpredicted by about 100 deg at 1 rad/s, although the prediction improves with increasing frequency until very good agreement is observed above 10 rad/s. At 120 kt the coherence is acceptably high only between about 2–20 rad/s. At 2 rad/s, the amplitude is overpredicted by about 5 dB with respect to the flight test data as shown in Fig. 13, but the prediction becomes much more accurate with increasing frequency. Much larger phase delays are predicted than are actually observed in flight. The discrepancy increases from about 100 deg at 3 rad/s to almost 200 at 20 rad/s.

Many additional results can be found in Ref. 15, including frequency response plots for off-axis response, and results showing the effects of several modeling and implementation assumptions such as 1) number of DOF, 2) choice of step size and type of finite difference approximations for the linearized model, and 3) choice of method to average the azimuth dependent linearized system matrices in forward flight.

Several frequency response plots presented here show rather large discrepancies for frequencies below 1–2 rad/s, the reasons for which are not entirely clear.

Dynamic inflow was found to have only a minor influence in the hover correlation study of Ref. 3, and is not likely to make a significant impact in forward flight, at low frequencies. Similarly, the results obtained using a model of the propulsion system, shown in all the frequency response plots, indicate that the lack of modeling of the rotor speed DOF is not a major contributor to the discrepancies. This, despite the fact the propulsion system has poles in the frequency band below 2 rad/s.[21] It is possible that unmodeled aerodynamic interactions between the main rotor wake and the tail rotor may cause errors in the predictions. Because of the canted tail rotor configuration, errors in tail rotor modeling can affect the longitudinal, as well as the lateral-directional dynamics. Curtiss[22] has shown that a simple interaction model based on a flat wake representation can considerably improve the accuracy of the predicted response to pedal inputs. Neglecting the main rotor/tail rotor interaction seems to lead to an overprediction of the response both for the on-axis, yaw response and the off-axis, pitch and roll responses, and most of the low-frequency errors shown in Figs. 6–13. It is also possible that the relatively crude modeling of the elastic torsion of the main rotor blades may account for some of the low-frequency errors. The blade torsional frequencies are well above the frequency range of interest. However, an inaccurate prediction of the steady-state torsional deformations of the blade may cause errors in the distribution of the aerodynamic loads over the rotor disk, and therefore, in the evaluation of pitching and rolling moments.

Conclusions

The purpose of this article was to introduce an algorithm for trim calculations in forward flight, including rotor dynamics, and to present the results of a validation study for a high-order linearized model of helicopter flight dynamics, and for a forward flight condition. Based on the results presented, several conclusions may be drawn. These conclusions refer to an articulated rotor helicopter.

1) The trim algorithm is numerically very accurate. When both phases of the algorithm are carried out, numerical simulations of the fixed-stick response from trim show that the aircraft states do indeed remain at their trim value for extended periods of time. The first phase of the trim procedure, without the subsequent refinement, provides sufficiently accurate solutions in most cases. The predictions of fuselage attitudes and pitch control settings agree well with flight test data, except at advance ratios lower than $\mu = 0.1$.

2) The trim algorithm provides the steady-state, periodic response of the rotor blades, and captures the periodicity of both rotor and fuselage states. Therefore, the algorithm can be useful for both flight dynamics and rotor dynamics or aeroelasticity applications.

3) Overall, the on-axis response predictions of the linearized simulation model are in good agreement with flight test results for frequencies above 1–2 rad/s. Fair agreement is obtained in the heave DOF. Several features associated with rotor dynamics are also captured correctly. Therefore, the model may represent a useful tool for the design of advanced flight control systems and for the prediction of compliance with handling qualities specifications.

4) Some discrepancies in the low-frequency correlation require further study. Improved predictions may require a more refined treatment of the aerodynamic interactions between the main rotor and the tail rotor.

Acknowledgments

This work was funded by the U.S. Army Aeroflightdynamics Directorate, Ames Research Center, through NASA-University Consortium NCA2-S11. The authors wish to thank Mark G. Ballin for his help with the Genhel computer program, and Jay W. Fletcher for providing the frequency response flight test data.

References

[1]Key, D. L., and Hoh, R. H., "New Handling-Qualities Requirements and How They Can Be Met," *Proceedings of the 43rd Annual Forum of the American Helicopter Society*, St. Louis, MO, May 1987, pp. 975–990.

[2]Kim, F. D., Celi, R., and Tischler, M. B., "High-Order State Space Simulation Models of Helicopter Flight Mechanics," *Proceedings of the Sixteenth European Rotorcraft Forum*, Glasgow, Scotland, UK, Sept. 1990.

[3]Ballin, M. G., and Dalang-Secretan, M.-A., "Validation of the Dynamic Response of a Blade-Element UH-60 Simulation Model in Hovering Flight," *Journal of the American Helicopter Society*, Vol. 36, No. 4, 1991, pp. 77–88.

[4]Kaplita, T. T., Driscoll, J. T., Diftler, M. A., and Wong, S. W., "Helicopter Simulation Development by Correlation with Frequency Sweep Flight Test Data," *Proceedings of the 45th Annual Forum of the American Helicopter Society*, Boston, MA, May 1989, pp. 681–692.

[5]Howlett, J. J., "UH-60A Black Hawk Engineering Simulation Program—Volume II—Background Report," NASA CR-166310, Dec. 1981.

[6]Peters, D. A., Kim, B. S., and Chen, H.-S., "Calculation of Trim Settings of a Helicopter Rotor by an Optimized Automatic Controller," *Journal of Guidance, Control, and Dynamics*, Vol. 7, No. 1, 1984, pp. 85–91.

[7]Peters, D. A., Chouchane, M., and Fulton, M., "Helicopter Trim with Flap-Lag-Torsion and Stall by an Optimized Controller," *Journal of Guidance, Control, and Dynamics*, Vol. 13, No. 5, 1990, pp. 824–834.

[8]Peters, D. A., and Izadpanah, A., "Helicopter Trim by Periodic Shooting with Newton-Raphson Iteration," *Proceedings of the 37th Annual National Forum of the American Helicopter Society*, Paper 81-23, Washington, DC, May 1981.

[9]Chen, R. T. N., and Jeske, J. A., "Kinematic Properties of the Helicopter in Coordinated Turns," NASA TP 1773, April 1981.

[10]Celi, R., "Hingeless Rotor Dynamics in Coordinated Turns," *Journal of the American Helicopter Society*, Vol. 36, No. 4, 1991, pp. 39–47.

[11]Takahashi, M. D., and Friedmann, P. P., "Active Control of Helicopter Air Resonance in Hover and Forward Flight," *Proceedings of the AIAA/ASME/ASCE/AHS 29th Structures, Structural Dynamics and Materials Conference*, Williamsburg, VA, Sept. 1988, pp. 1521–1532.

[12]Lim, J. W., Chopra, I., "Stability Sensitivity Analysis for Aeroelastic Optimization of a Helicopter Rotor," *AIAA Journal*, Vol. 28, No. 6, 1990, pp. 1089–1097.

[13]Pitt, D. M., and Peters, D. A., "Theoretical Prediction of Dynamic Inflow Derivatives," *Vertica*, Vol. 5, No. 1, 1981, pp. 21–34.

[14]Celi, R., "Effects of Hingeless Rotor Aeroelasticity on Helicopter Longitudinal Flight Dynamics," *Journal of the American Helicopter Society*, Vol. 36, No. 2, 1991, pp. 35–44.

[15]Kim, F. D., "Formulation and Validation of High-Order Mathematical Models of Helicopter Flight Dynamics," Ph.D. Dissertation, Dept. of Aerospace Engineering, Univ. of Maryland, College Park, MD, Sept. 1991.

[16]Abbott, W. Y., Benson, J. O., Oliver, R. G., and Williams,

R. A., "Validation Flight Tests of UH-60A for Rotorcraft Systems Integration Simulator (RSIS)," U.S. Army Aviation Engineering Flight Activity, 79-24, July 1982.

[17]Ballin, M. G., "Validation of a Real-Time Engineering Simulation of the UH-60A Helicopter," NASA TM-88360, Feb. 1987.

[18]Tischler, M. B., and Cauffman, M. G., "Frequency-Response Method for Rotorcraft System Identification with Applications to the Bo-105 Helicopter," *Journal of the American Helicopter Society*, Vol. 37, No. 3, 1992, pp. 3–17.

[19]Tischler, M. B., "Frequency-Response Identification of XV-15 Tilt-Rotor Aircraft Dynamics," NASA TM-89428; see also U.S. Army Aviation Systems Command TM 87-A-2, May 1987.

[20]Kim, F. D., "Analysis of Propulsion System Dynamics in the Validation of a High-Order State Space Model of the UH-60," *Proceedings of the 1992 AIAA/AHS Flight Simulation Technologies*, Hilton Head, SC, Aug. 1992.

[21]Ballin, M. G., "A High Fidelity Real-Time Simulation of a Small Turboshaft Engine," NASA TM-100991, July 1988.

[22]Curtiss, H. C., Jr., and Quackenbush, T. R., "The Influence of the Rotor Wake on Rotorcraft Stability and Control," *Proceedings of the Fifteenth European Rotorcraft Forum*, Amsterdam, The Netherlands, Sept. 1989.